Bioactive Materials 8 (2022) 381–395

Contents lists available at ScienceDirect

Bioactive Materials

journal homepage: www.sciencedirect.com/journal/bioactive-materials

Anti-infection mechanism of a novel dental implant made of titanium-copper (TiCu) alloy and its mechanism associated with oral microbiology

Hui Liu [a,b,1], Yulong Tang [c,1], Shuyuan Zhang [b], Huan Liu [a,b], Zijian Wang [c], Yue Li [c], Xinluan Wang [d,e], Ling Ren [b,*], Ke Yang [b,**], Ling Qin [d,e,***]

[a] School of Materials Science and Engineering, University of Science and Technology of China, 96 Jinzhai Road, Hefei, 230026, China
[b] Shi-changxu Innovation Center for Advanced Materials, Institute of Metal Research, Chinese Academy of Sciences, 72 Wenhua Road, Shenyang, 110016, China
[c] Department of Stomatology, General Hospital of Northern Military Area, 83 Wenhua Road, Shenyang, 110016, China
[d] Translational Medicine R&D Center, Institute of Biomedical and Health Engineering, Shenzhen Institutes of Advanced Technology, Chinese Academy of Sciences, Shenzhen, 518057, China
[e] Musculoskeletal Research Laboratory of Department of Orthopaedics & Traumatology and Innovative Orthopaedic Biomaterial and Drug Translational Research Laboratory of Li Ka Shing Institute of Health, The Chinese University of Hong Kong, Hong Kong Special Administrative Region of China

ARTICLE INFO

Keywords:
Titanium-copper alloy implants
Anti-infection
Oral microbiology
Biosafety

ABSTRACT

This work was focused on study of anti-infection ability and its underlying mechanism of a novel dental implant made of titanium-copper (TiCu) alloy. In general, most studies on antibacterial implants have used a single pathogen to test their anti-infection ability using infectious animal models. However, dental implant-associated infections are polymicrobial diseases. We innovatively combine the classic ligature model in dogs with sucrose-rich diets to induce oral infections via the canine native oral bacteria. The anti-infection ability, biocompatibility and underlying mechanism of TiCu implant were systematically investigated in comparison with pure Ti implant via general inspection, hematology, imageology (micro-CT), microbiology (16S rDNA and metagenome), histology, and Cu ion detections. Compared with Ti implant, TiCu implant demonstrated remarkable anti-infection potentials with excellent biocompatibility. Additionally, the underlying anti-infection mechanism of TiCu implant was considered to involve maintaining the oral microbiota homeostasis. It was found that the carbohydrates in the plaques formed on the surface of TiCu implant were metabolized through the tricarboxylic acid cycle (TCA) cycles, which prevented the formation of an acidic microenvironment and inhibited the accumulation of acidogens and pathogens, thereby maintaining the microflora balance between aerobic and anaerobic bacteria.

1. Introduction

Dental implants are a popular option for replacing the missing teeth [1]. Globally, 10 million dental implants are used annually for clinical treatments [2]. However, implant-associated infections remain critical challenges clinically. Approximately 80% of patients with implants were reported to experience peri-implant mucositis, and peri-implantitis occurred in 28–77% of patients [3]. The major causes for these infections are the faster microbial biofilm formation compared to the tissue integrations on the surface of the implants [4]. In the oral environment, microorganisms from oral fluids easily attach to the implant surfaces, including saliva and gingival crevicular fluid. Then a firm layer of bacteria accumulates together with the secreted glycoproteins and polysaccharides, known as biofilms [5]. Biofilms,

Peer review under responsibility of KeAi Communications Co., Ltd.
* Corresponding author.
** Corresponding author.
*** Corresponding author. Musculoskeletal Research Laboratory of Department of Orthopaedics & Traumatology and Innovative Orthopaedic Biomaterial and Drug Translational Research Laboratory of Li Ka Shing Institute of Health, The Chinese University of Hong Kong, Hong Kong Special Administrative Region of China.
E-mail addresses: lren@imr.ac.cn (L. Ren), Kyang@imr.ac.cn (K. Yang), lingqin@cuhk.edu.hk (L. Qin).
[1] These authors contributed equally to this work.

https://doi.org/10.1016/j.bioactmat.2021.05.053
Received 20 April 2021; Received in revised form 19 May 2021; Accepted 30 May 2021
Available online 16 June 2021

especially those containing pathogens, may lead to persistent peri-implant infections [6]. Hence, one ideal strategy to combat implant-associated infections would be the introduction of antibacterial actions to implant design and fabrication, including delivery of antibiotics or metal ions through implant surfaces [7,8] or antibacterial alloys [9,10]. Previously, we developed a multi-functional titanium copper (TiCu) alloy with both osteogenic and antibacterial potentials [11]. TiCu alloy effectively inhibited biofilm formation *in vitro*, showing 99.5% and 90.0% antibacterial rates against *S. aureus*, a known orthopedic pathogen [12], and *S. mutans*, an oral pathogen [13], respectively. Another preliminary *in vivo* study also confirmed that the surfaces of TiCu implants possessed excellent anti-infective and osteogenic abilities [14].

Considerable number of researchers have been focusing on exploring the anti-infective functions of the implants in animal models. The anti-infection ability of Zn-Cu nails immersed with methicillin-resistant *Staphylococcus aureus* was evaluated in rat femurs [10]. Ciprofloxacin-containing coatings on the porous titanium was implanted with *P. aeruginosa* in murine subcutaneous tissues to examine the infection [15]. Zhou et al. used tubercle bacilli to induce osteoarticular tuberculosis disease in New Zealand rabbits and tested the therapeutic efficacy of the drug-releasing hydroxyapatite scaffolds [16]. However, these single-pathogen models were in vain to reveal the effect of diverse oral microbiome on peri-implant infections. Especially, oral cavity contains over 700 bacterial species [17], and peri-implant infections are polymicrobial diseases, closely associated with the homeostasis of the oral microbiota [18]. Additionally, the dysbiosis of oral microbiota may induce not only diseases in the mouth, such as oral squamous cell carcinoma [19], but also systemic diseases, including diabetes and cardiovascular diseases [20]. Thus, it is highly desirable or more meaningful to establish a native oral infective environment in order to evaluate the effect of anti-infective implants on the oral microbiota [21].

16S rRNA gene sequencing and metagenomic analysis have been widely used to analyze the bacterial composition, diversity, and metabolism of oral microbiota. A previous study demonstrated that by16S rRNA gene sequencing the diversity of oral bacterial communities increased with the progression of peri-implant diseases [22]. Metagenomic analysis [23] was used to confirm that caries should be a polymicrobial disease related to interactions among *Parvibaculum*, *Syntrophus* and *Treponema*. The ligature-induced peri-implant lesions model has been a classic animal model to explore the effect of biofilm accumulations on clinical measures, such as bleeding and bone resorptions [24]. Moreover, increasing dietary sugars also threatens both oral and systemic health [25]. Among them, frequent consumptions of sucrose dramatically influence the biofilm development by the productions of extracellular polymeric substances, which are key components in biofilms [5]. For instance, sucrose can be fermented by *Streptococcus mutans* to acidify the biofilms [26]. To sum up, with the help of these advanced sequencing technologies, the combination of sucrose-rich diets and the ligature model makes it possible to objectively disclose the anti-infection mechanism of TiCu implant in the oral infective animals.

In this study, we creatively establish an oral infectious environment to investigate the anti-infection ability of TiCu implants through the bacteria endogenous in canine oral, the ligature model, and sucrose-rich diets, then 16S rRNA gene sequencing and metagenomics were performed to explore the anti-infection mechanism and the biosafety of TiCu implants. The results of this study provided a new knowledge to understand the anti-infection mechanism of the antibacterial metal implants.

2. Materials and methods

2.1. Preparation of TiCu implant

TiCu alloy was melted in a vacuum consumable furnace with a nominal composition of Ti-5 wt.% Cu, and the ingot was deformed into a bar with diameter of 4 mm at 850 °C and annealed at 740 °C. Under this processing, TiCu alloy with microstructure of α-Ti + Ti_2Cu assessed the best superior strength and plasticity as well as good corrosion resistance and antibacterial activity reported recently by our group [11,27], whose elongation of can reach up to 26%, and the tensile strength of Ti-5 wt.% Cu alloy with 740 °C heat treatment is up to 600 MPa, both far higher than pure titanium at TA2 level according to GB/T 13810-2017. The bar was machined into 24 implants (ϕ3.6 mm × 8 mm) and achieved by sandblasted with large grift and acid etching (SLA) treatment. Finally, TiCu implants were cleaned with ethanol and sterilized with ethylene oxide. The same size clinical implants made of commercial pure titamium were chosen as a control group (Dentium, Korea) in all the experiments, named as Ti implant. The surface morphologies and roughness of the Ti and TiCu implants were measured by a scanning electron microscope (SEM, SHIMADZU SSX-550, Japan) and the profilometer (Micro XAM, KLA-Tencor, USA), respectively. The diameters of the holes on the implant surfaces were analyzed from the SEM images by Image J software, then the mean values are determined as the hole diameters.

2.2. Surgical procedure

The animal protocol was approved by the Animal Ethics Committee of Shenzhen Advanced Animal Study Service Center (Shenzhen, China, Accreditation ID: AAS190105D-01 and AAS190106D-01). Twelve male beagles (1 year old, 13–15 kg) with healthy oral cavities were randomly divided into four groups (each group with 3 dogs). Therein, two groups of animals were respectively implanted with Ti implants and TiCu implants in the ligature and sucrose-rich diet model (i.e., infection model). The infection model was used to assess the anti-infection abilities of TiCu implants associated with the microbiology of plaque microbiota, which was the focus of this work. The other two groups of animals were respectively utilized to further verify the biosafety of Ti and TiCu implants and their effects on the saliva microbiome in the normal implantation model.

Briefly, all the animals underwent extractions of first to fourth premolars in the bilateral mandibular, and three months later, implantation surgeries were performed. All the surgical procedures were proceeded under inhalation anesthesia with a mix of oxygen, nitrous oxide and isoflurane.

Fig. 1a_1 presents the implantation diagram in the infection model, each dog had 2 implants placed in the healed extraction sites on the unilateral mandible (Fig. 1a_2), the neck of implants was 1.5-mm-depth below the bone crest. Subsequently, healing abutments (Dentium, Korea) were screwed to the implants (Fig. 1a_3) and cotton floss was ligatured around the abutments, one floss end was exposed in the oral and the other end was sheltered under the flaps. The flaps were sutured and the abutments were exposed (Fig. 1a_4). These animals were fed with the soft diets containing sucrose (500 g per day). Two weeks after implantations the sutures were removed. All the animals were routinely monitored for swelling, dehiscence, and infection, supragingival and subgingival plaques were collected monthly.

Fig. 1b_1 shows the implantation diagram in the normal implantation model, after the same implantation method as described in the infection model, implants were sealed by cover screws (Dentium, Korea) to avoid peri-implant infections (Fig. 1 b_2 and b_3). The soft tissues were sutured over the screws and implants (Fig. 1b_4). These animals were fed with normal soft food. Saliva was obtained after three months as the screws were below the tissues.

Three months after implantations, all animals were sacrificed, the mandibles and main organs were harvested and immersed in 10% formalin for subsequent analysis, including brain, lung, heart, liver, spleen, and kidney.

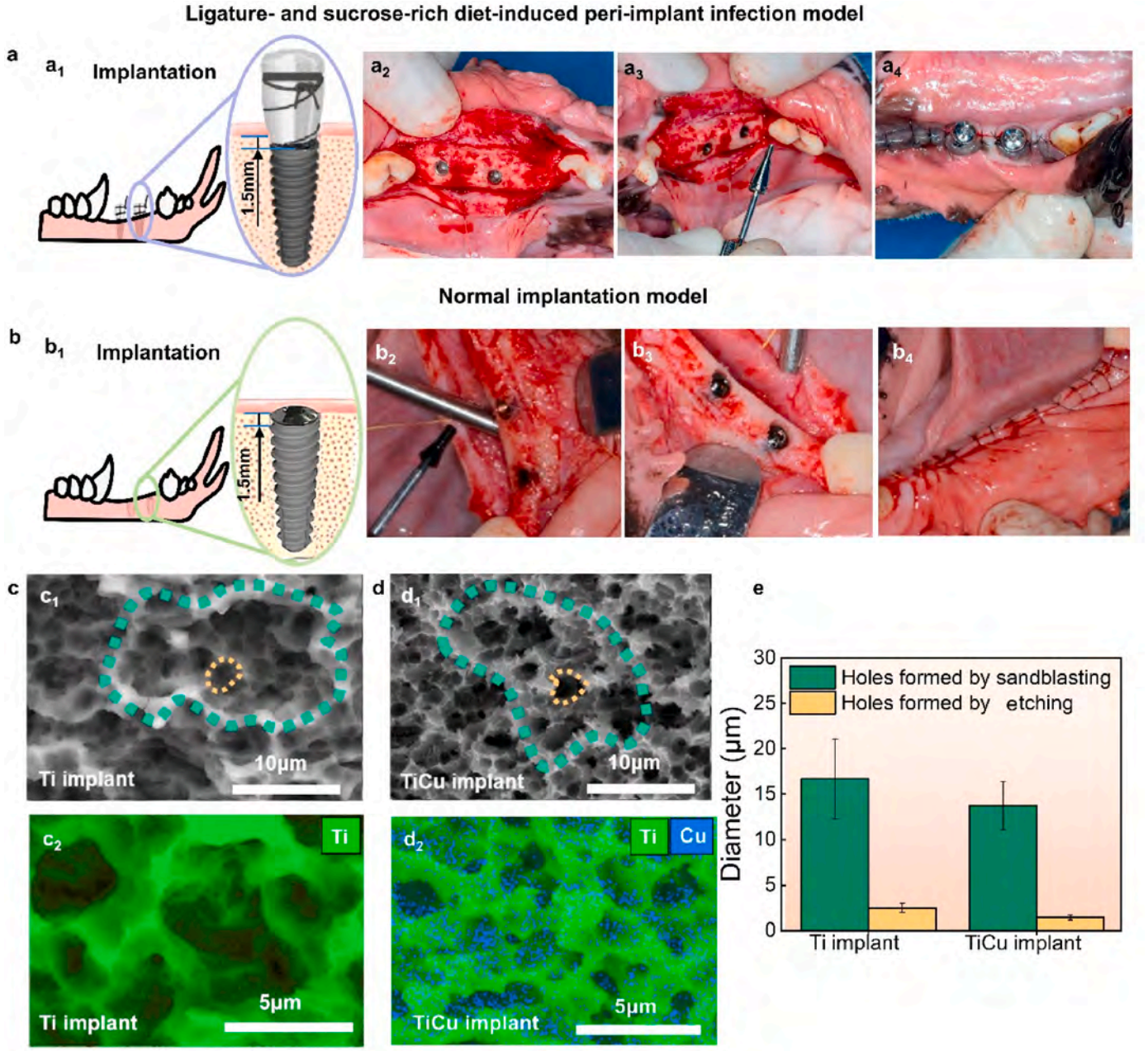

Fig. 1. Implantation surgical procedures and surface characters of implants. (a) For the animals in ligature and sucrose-rich diet-induced peri-implant infection model, four same implants were inserted into the dog mandible (a_1 and a_2, two implants/side), the healing abutments were applied with ligatures (a_3), and then the flaps sutured through the abutments(a_4), these animals were then fed on sucrose-rich diets. (b) In normal implantation model, four same implants were also inserted into the mandible (b_1 and b_2, two implants/side), cover screws were used after implantations(b_3), the flaps were sutured over the screws and implants(b_4), and these animals were fed normal diets. (c_1) and (d_1) Surface morphologies of Ti and TiCu implants, green rings indicate the holes formed by sandblasting treatment and the yellow rings show the holes formed by acid etching treatment. (c2) and (d_2) EDS surface scanning images of Ti and TiCu implants, respectively. (e) Diameters of holes on the implant surfaces. (n = 3 per group) [Data are mean ± s.d.].

2.3. Micro-computed tomography analysis

To visualize the peri-implant bone tissues in the infection model and the normal implantation model, the harvested mandible specimen underwent micro-computed tomography analysis (micro-CT, Aartselaar, Belgium) with a resolution of 18 μm at 65 kV and 385 μA. Magnified images of implants were obtained by selecting region of interest (ROI) around the tissues. The ROI region was defined as a cylinder with a radius of 360 μm from the implant surface and a height of 6 mm. Qualitative analysis of the trabecular thickness (Tb. Th), trabecular number (Tb. N), trabecular separation (Tb. Sp), bone volume/tissue volume (BV/TV), and bone surface/bone volume (BS/BV) was performed using built-in software.

2.4. Histopathological analysis

In the infection model, the formalin-fixed mandibles were dissected using a diamond saw (Buehler, USA) and processed for ground sectioning [13], then these mandibles were embedded in Technovit 4000 VLC-resin (Kulzer, Friedrichsdorf, Germany) and cut in a buccal-lingual direction using a cutting grinding unit (Exakt, Apparatebau, Norderstedt, Germany). From each block, two buccal-lingual

sections including the implant were prepared. All the sections were reduced to a thickness of 10 μm by micro-grinding and polishing using a micro-grinding unit (Buehler, USA). The formalin-fixed main organs were dehydrated and embedded in paraffin, including brain, lung, heart, liver, spleen, and kidney, which were then sectioned by a microtome (Buehler, USA) with thickness of 8 μm. Organs and mandibles sections were all stained with hematoxylin and eosin (H&E) (Sbjbio, China) for general observation and analysis. Briefly, sections were treated with hematoxylin for 20 min and eosin solution for 20 min and then visualized on an optical microscope (ZEISS, Germany). Evaluations focused on the following aspects, including chronic intraosseous inflammation, acute intraosseous inflammation, bone resorption and bone destruction, with regards to TiCu implants on the peri-implant tissues. Analysis was conducted in a blinded manner based on an established scoring system with identical modifications [28,29]. Briefly, two experienced examiners independently performed the histopathologic evaluation including the above four factors, each factor was scored from 0 to 4 points, and the histological score was calculated by adding four scores. Higher score indicated a more severe peri-implant infection. When consensus between the two examiners was not achieved, an independent examiner reviewed the histological findings to reach a final decision, the examiners masked with regard to the implantation rendered to the extent possible.

For the osseointegration assay, mandibles specimens were sequentially immersed in methylene blue and acid fuchsin (Sbjbio, China) for 10 min. The images were observed on the optical microscope (ZEISS, Germany). Bone-implant contact (BIC, %) rate was calculated as the ratio of the length of the implant profile in direct contact with the bone surface to the total length of the implant profile [13].

2.5. Blood collection and cytokine assay

In the infection model, 50 mL blood was collected monthly from the forelimb veins of beagles and stored in serum gel tubes. Some fresh blood samples were directly used to assess the level of leukocytes by a blood cell count analyzer (Erba Msnnheim, UK). Other samples were centrifuged for 10 min at 3000 rpm at 4 °C in order to collect the serum for analysis of copper ions and cytokines, including interleukin (IL)-6, tumor necrosis factor-α (TNF-α) and procalcitonin (PCT). IL-6 and TNF-α were tested in a multiplex analyzer (Bio-Rad Laboratories, USA), and PCT was analyzed via the immune analyzer (Roche, Germany) according to the manufacturer's instructions.

2.6. Copper distribution in blood and peri-implant tissues

The copper concentrations in the serum and organs in the two group animals were measured by atomic absorption spectrometry (AAS, Agilent, USA) for evaluating distribution of released copper ions from TiCu implant *in vivo*. Furthermore, in the normal implantation model, the copper content in the peri-implant bones was also measured to further analyze the effect of TiCu implant on the bone tissues. 3-mm width of bone tissues surrounding the implants were harvested to measure the copper content by AAS.

2.7. Effects of TiCu implant on the oral microbiota

To reveal the effects of TiCu implant on the oral microbiome in different models, 16S rRNA gene sequence technology was used to analyze the microbiota compositions, and metagenomic analysis was chosen to study the metabolism of oral microbiota. In consideration of the implantation difference in two models, dental plaques were collected in the infection model to further explore the anti-infection mechanism of TiCu implant, and saliva was collected in the normal implantation model to evaluate the biosafety of TiCu implant for oral applications.

2.7.1. Oral sample collection and microbial DNA extraction

Collection of oral samples followed the standard collection procedures as set forth by the Human Microbiome Project [30] with proper adjustments under general anesthesia. In the normal implantation model, saliva was collected by natural discharge into a centrifuge tube (5 mL per dog) three months after implantations. For the dogs in the infection model, plaques around the ligatures of the healing abutment and subgingival plaques were collected monthly using plastic loops to avoid blood contaminations. All oral samples were stored at −80 °C until the DNA extractions in BGI Research (BGI, Shenzhen, China). Microbial genomic DNA was extracted by the epicentre masterpure gram positive DNA purification kit (Epicentre, USA). The quantity of genomic DNA was measured by qubit dsDNA BR assay kit (Invitrogen, USA), and the quality was verified on 1% agarose gel.

2.7.2. 16S rRNA gene sequence and data analysis

The V4 region of 16S rRNA gene was amplified from the DNA extractions with degenerate PCR primers 515F (5′-GTGCCAGCMGCCGCGGTAA-3′) and 806R (5′-GGACTACHVGGGTWTCTAAT-3′), and each primer was modified with Illumina adapter, pad, and linker sequences. PCR enrichment was performed in a total reaction volume of 50 μL containing: 30 ng DNA, fusion PCR primer and PCR master mix (Applied Bioscience, USA), which was incubated at 98 °C for 30 s, followed by 30 cycles of 98 °C (15 s), 58 °C (15 s), 72 °C (15 s) and a final elongation at 72 °C (60 s). The 16S amplicons were purified with agencourt AMPure XP-Medium kits (Beckman, USA). Finally, 2 × 250 bp paired-end reads were generated by sequencing on an Illumina HiSeq 2500 platform (Illumina, USA).

Following sequencing, raw reads shorter than 300 bp and any remnant primer sequences were trimmed away, and then high-quality paired-end reads were clustered into the operational taxonomic units (OTUs) at a similarity level of 97%. The taxonomic classification of OTUs was performed using Greengenes database (version 201305) on Ribosomal Database Project (RDP, version 2.2) Classifier. Species compositions were created using GraPhlAn (http://www.graphpad.com), heatmap analysis at phylum level was plotted with R software (https://www.r-project.org/). Alpha diversity was estimated by MOTHUR [31]. Linear discriminant analysis Effect Size (LEfSe, https://huttenhower.sph.harvard.edu/galaxy/) was used to identify the significant difference of species associated with Ti or TiCu implants, and spearman correlations of those different species were also analysis using R software.

2.7.3. Metagenomic sequences and data analysis

Genomic DNA was randomly fragmented by a focused-ultrasonicator (Covaris, USA). DNA fragments, 200–400 bp in size on average, were selected by magnetic beads, then end-repaired, 3' adenylated, and ligated to adapters. After PCR amplification and purification, single strand circle DNA was obtained by heat denaturing and formatted as the final library. The qualified libraries were sequenced on BGISEQ-500 (BGI, China). High-quality reads were trimmed by SOAPnuke [32] and assembled de-novo using Megahit software (https://github.com/voutcn/megahit). Genes were predicted over contigs by using MetaGeneMark (version 2.10), and redundant genes were removed using CD-HIT [33]. The gene sequences were aligned against the Kyoto Encyclopedia of Genes and Genomes database (KEGG, version 89.1) by DIAMOND with an E value cutoff of 1e-5. The different KEGG pathways in the microflora associated with Ti or TiCu implants were identified according to reporter scores (Ti: scores < -1.65, TiCu: scores > 1.65). Meanwhile, the sequences were aligned against the Antibacterial Biocide & Metal Resistance Genes Database.

2.8. Data and materials availability

All the data needed to evaluate the conclusions were present in the study. Illumina paired-end raw reads of 16S rRNA gene sequences and BIGSEQ paired-end raw reads of metagenomic sequences analyzed for

this study were deposited in the NCBI's Sequence Read Archive (SRA) database under accession number (SUB8712988 and SUB8713343) and BioProject (PRJNA684049 and PRJNA684764), respectively.

2.9. Statistical analysis

All the morphological, physiological, micro-CT and histomorphometric results were analyzed using Student's *t*-test in the SPSS software (SPSS Inc., USA). Three dogs were allocated to each group in the experiments for statistical analysis. The results were presented as the mean ± standard deviation. Additional statistical analysis was done using R software (version 3.4.1), and Wilcoxon rank-sum test and various packages were used to value the effects of Ti and TiCu implants on the plaque and saliva microbiology. The results were considered statistically significant at * $P < 0.05$, ** $P < 0.01$, and *** $P < 0.001$.

3. Results

3.1. Surface characterizations

As shown in Fig. 1c and d, both commercial Ti and TiCu implants showed typical SLA topographies with honeycomb-like holes. The diameters of sandblasting holes and etching cavities on both implants were similar, ranging in 10–20 μm and 1–3 μm, respectively (Fig. 1e). The Cu element centralized around the etching cavities on the surface of TiCu implant (marked by the blue points in Fig. 1d_2). The surface roughness of Ti and TiCu implants was respectively 1.57 ± 0.82 μm and 2.01 ± 0.18 μm without significant differences, which were optimum roughness of implants with strong bone responses [34].

3.2. Ligature and sucrose-rich diet-induced infection model

In this work, we induce peri-implant infection by native oral microbiota in order to assess the anti-infective ability and biosafety of TiCu implants, including visual observations, histopathological analysis, blood leukocyte analysis, cytokine analysis, and released Cu content evaluation. Moreover, the effect of TiCu implants on the plaque microbiology was explored by 16S rDNA and metagenomic sequencings to study the underlying anti-infective mechanism.

3.2.1. Visual inspection

Visual inspection was designed to analyze the inflammatory responses of the peri-implant soft tissues (Fig. 2a). Gingival tissues around Ti implants were infected by swelling at 1 month (1 M), and bleeding on probing (BOP) at 2 month (2 M) and 3 month (3 M) as marked by the yellow arrows. In contrast, the tissues surrounding the TiCu implants were healthy with normal appearance and no BOP. All implants adhered firmly with the bones.

3.2.2. H&E staining

To further reveal the anti-infection ability of TiCu implant, H&E staining was used to observe the peri-implant tissues. Histological score of TiCu group was significantly lower than that of Ti group (Fig. 2b), which indicated the excellent anti-infection ability of TiCu implant.

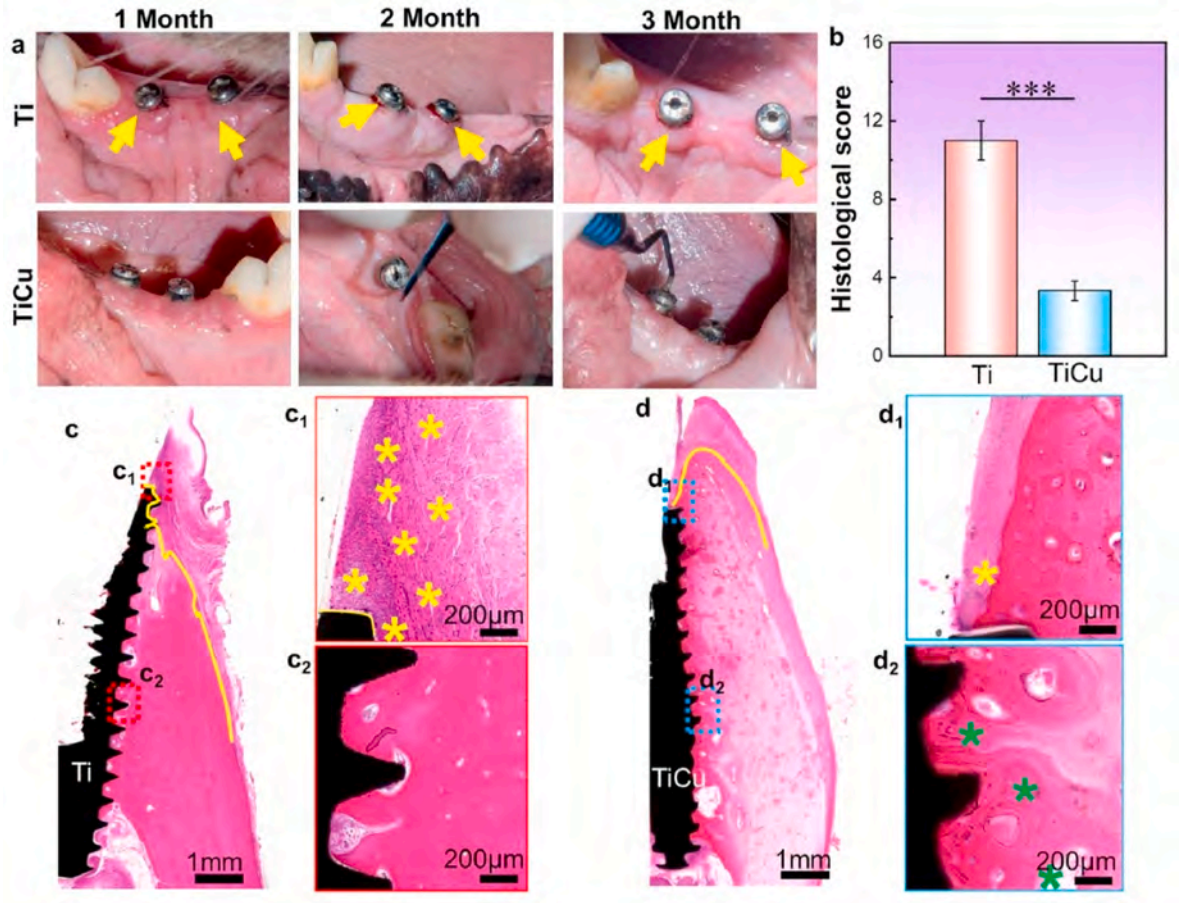

Fig. 2. Anti-inflammatory analysis of Ti and TiCu implants in the infection model. (a) Visual inspections of gingival tissues surrounding Ti or TiCu implants, yellow arrows showing swelling and bleeding of the gums. (b) Statistical analysis of histological scores, *** $P < 0.001$. (c) and (d) H&E staining analysis of mandibles tissues around Ti or TiCu implants at 3 months. (c_1, c_2, d_1, and d_2) Local images of tissues surrounding the Ti or TiCu implants, yellow stars showing the inflammatory cells, and green stars showing the osteoblasts (n = 3 per group) [Data are mean ± s.d. and *** $p < 0.001$ compared with the pure Ti implant].

Besides, it was shown that apparent inflammatory cells and thick fibrous layers gathered in the soft tissues around Ti implant (yellow stars, Fig. 2c$_1$), and the fibrous tissues rather than bone tissues directly covered the neck of Ti implant (yellow lines, Fig. 2c). In contrast, slight inflammatory response (Fig. 2d$_1$) and more osteoblasts (green stars in Fig. 2d$_2$) distributed around TiCu implant. Meanwhile, the bone tissues completely covered the TiCu implant (yellow line in Fig. 2d), which also confirmed that TiCu implant could effectively inhibit the inflammatory reactions in the gingival tissues.

3.2.3. Micro-CT analysis

Micro-CT analysis is the most basic and intuitive method to assess peri-implant bone tissues, where bone is indicated by green color. Slightly bone resorption with depth of 1 mm was detected around the Ti implant (Fig. 3a$_1$). Furthermore, dense bone tissues surrounded the bodies of both types of implants. In the enlarged views (Fig. 3a$_2$ and 3b$_2$) where bone tissue was marked in red and implants were shown in grey, numerous bone tissues evenly covered the thread profiles of the TiCu implant, while fewer bone tissues heterogeneously distributed around the Ti implant, which indicated TiCu implant had a tendency to improve osseointegration. Quantitative analyses of micro-CT also confirmed the above detections, both Tb. N and BV/TV values of TiCu group showed a higher trend than those of Ti group (Fig. 3c and e), yet without significant differences ($P > 0.05$), indicating that both Ti and TiCu implants had similar osseointegration in the infection model.

3.2.4. Methylene blue and acid fuchsin staining

To observe the osseointegration of the bone-implant interface, methylene blue and acid fuchsin were performed. In Fig. 3g, newly formed bones (NB) intensively distributed on the grooves of Ti implant, while NB evenly surrounded the TiCu implant profiles and more obvious hydroxyapatite layers appeared at the implant/bone interface (orange arrows in Fig. 3h), besides TiCu implant had a higher BIC rate than Ti implants in Fig. 3i. These results also indicated TiCu implants had a tendency to improve osseointegration compared with clinical pure Ti implants.

Based on the above results, dogs inserted with Ti implants were diagnosed for peri-implant mucositis with BOP and severe inflammatory responses with less than 2 mm depth of bone resorption, and the continual development of peri-implant mucositis could eventually lead to failures of implantation [18,35]. In contrast, animals with TiCu implants were still healthy in the infection model. To explore the

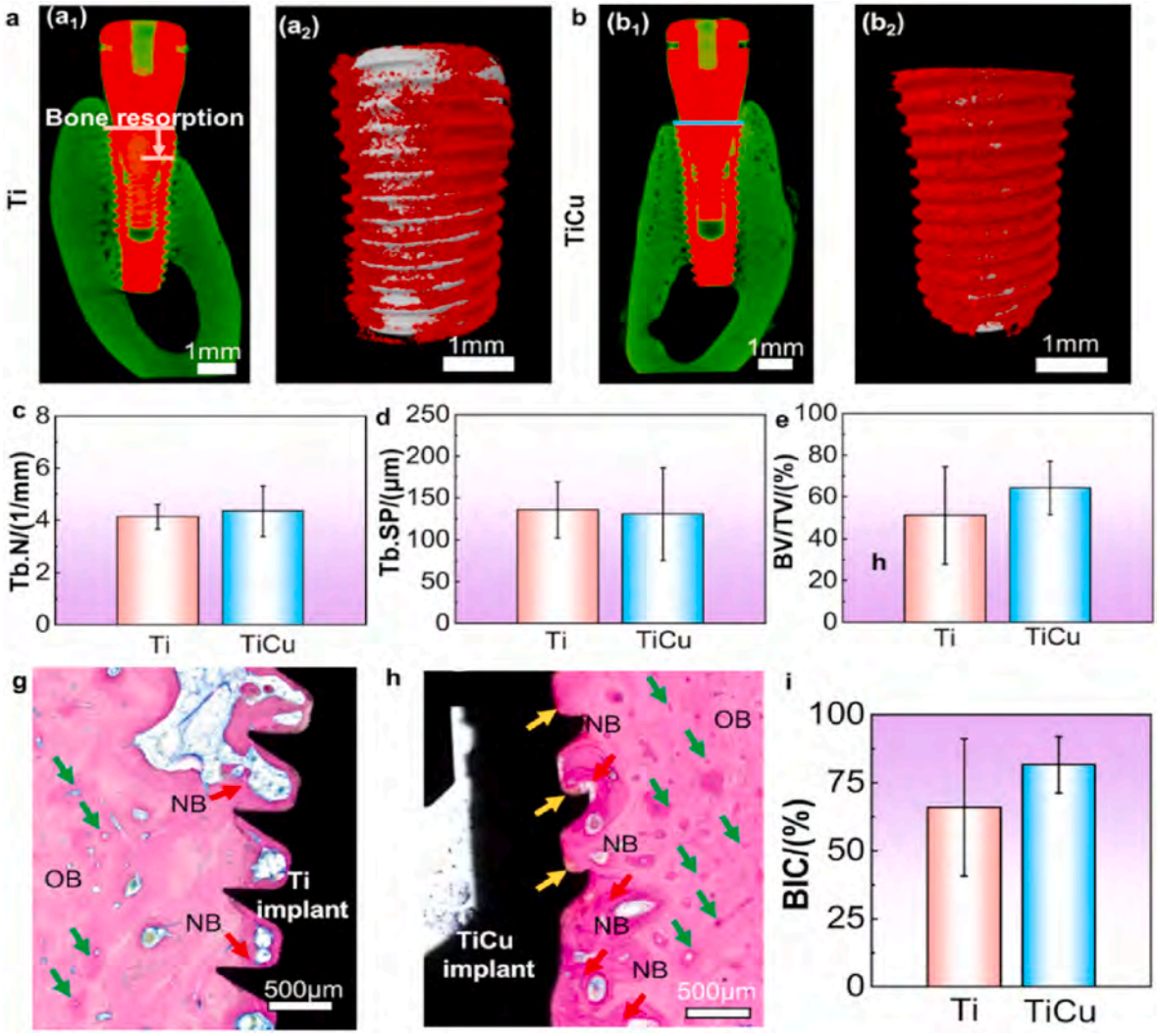

Fig. 3. Osseointegration analysis of Ti and TiCu implants in the infection model. (a$_1$) and (b$_1$) micro-CT images in the buccal-glossal direction, green color reflecting bone density. (a$_2$) and (b$_2$) enlarged images of Ti and TiCu groups, grey representing the implant, and red representing the bone tissues. Quantitative analysis of (c) trabecular number, (d) trabecular separation, (e) bone volume/tissue volume. (g) and (h)histological observations of the bone tissues around Ti and TiCu implants. OB: original bone; NB: newly formed bone marked by red arrows; yellow arrows show the hydroxyapatite layers, and green arrows show the Haversian system. (i) Bone implant contact rate (n = 3 per group) [Data are mean ± s.d. and *p < 0.05 compared with the pure Ti implant].

anti-infective mechanism of TiCu implants, the plaque microbiota was further analyzed, including species compositions and metabolic pathways.

3.2.5. Plaque microbial composition

In the infection model, 2,552,014 high-quality paired-end reads were obtained by 16S rRNA gene sequences and assigned to 631 OTUs. Based on the phylogenetic tree of seed sequences in Fig. 4a, the plaque microbiota on Ti and TiCu implant surfaces can be classified into 23 phyla, 42 classes, 61 orders, 92 families, and 150 genera. The dominant phyla (relative abundance >1%, Fig. 4b) included Bacteroidetes (50.5%), Firmicutes (15.5%), Proteobacteria (14.6%), Spirochaetes (3.5%), Synergistetes (3.3%), Actinobacteria (2.1%), and Chlorobi (1.9%) from 1 M to 3 M. However, Euryarchaeota and SR1 were only enriched in the plaque on the Ti implant. Plaque samples of Ti and TiCu groups at 1 M and 3 M were clustered together (Fig. 4b), indicating their similar microbial compositions. Therefore, the samples of 2 M and 3 M were selected to further analyze the significantly different genera.

Alpha diversity was also analyzed to reveal the effect of TiCu implant on plaque microbiome. In Fig. 4c and d, both observed species and Shannon indices revealed that TiCu implant had no effect on the diversity and richness of the oral microbiota.

3.2.6. Significant difference of genera in plaques attached on Ti and TiCu implant surfaces

In order to detect the microbial composition differences of Ti and TiCu groups, LEfSe analysis of microbiome profiles up to the genus level was performed. The endogenous genera in the Ti group at 2 M contained *VadinCA11*, *Oscillospira*, *Phascolarctobacterium*, *Oxalobacter*, *Bilophila* and *Sphaerochaeta* (green nodes, Fig. 4e). The plaque from the TiCu implant enriched *Filifactor* and *Bergeyella*, which were presented in red nodes. At 3 M, Ti implants accumulated more endogenous genera, including *VadinCA11*, *Blvii28*, *Lactobacillus*, *Streptococcus*, *Desulfobulbus*, *Campylobacter* and *Pasteurella* (Fig. 4f). *Prevotella*, *Catonella* and *p-75-a5* were the significant genera in the TiCu group.

Correlation analysis of the endogenous genera attached to Ti and TiCu implants was also performed in Fig. 5a and b, which was calculated via the relative abundances of those genera in all the samples. Positive correlations were observed among the genera in each group and were indicated with red circles. However, negative correlations were found

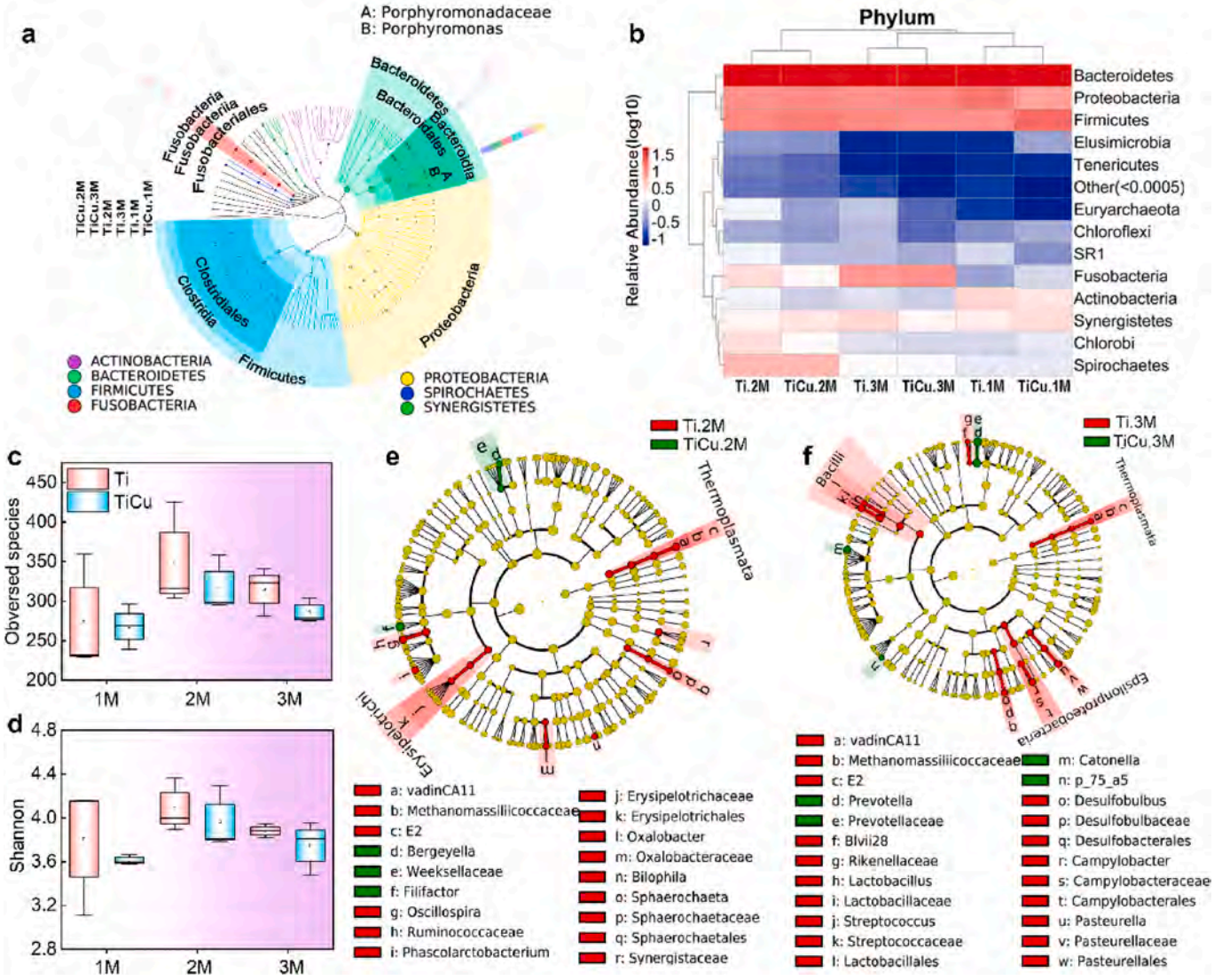

Fig. 4. Dental plaque microbiome compositions in the infection model. (a) Species composition tree, colorful circles showing the richest phyla in all samples and colorful peripheral rings representing the relative abundance of taxonomic microflora of Ti and TiCu groups from 1 M to 3 M. (b) Heatmap analysis at the phylum level, "Others" representing the sum of species whose abundance was less than 0.5% in all samples. Alpha diversity analyses of (c) Observed species and (d) Shannon indexes. (e) and (f) LEfSe analysis of microbiome profiles up to the genus level at 2 M and 3 M, respectively (n = 3 per group) [Data are mean ± s.d.].

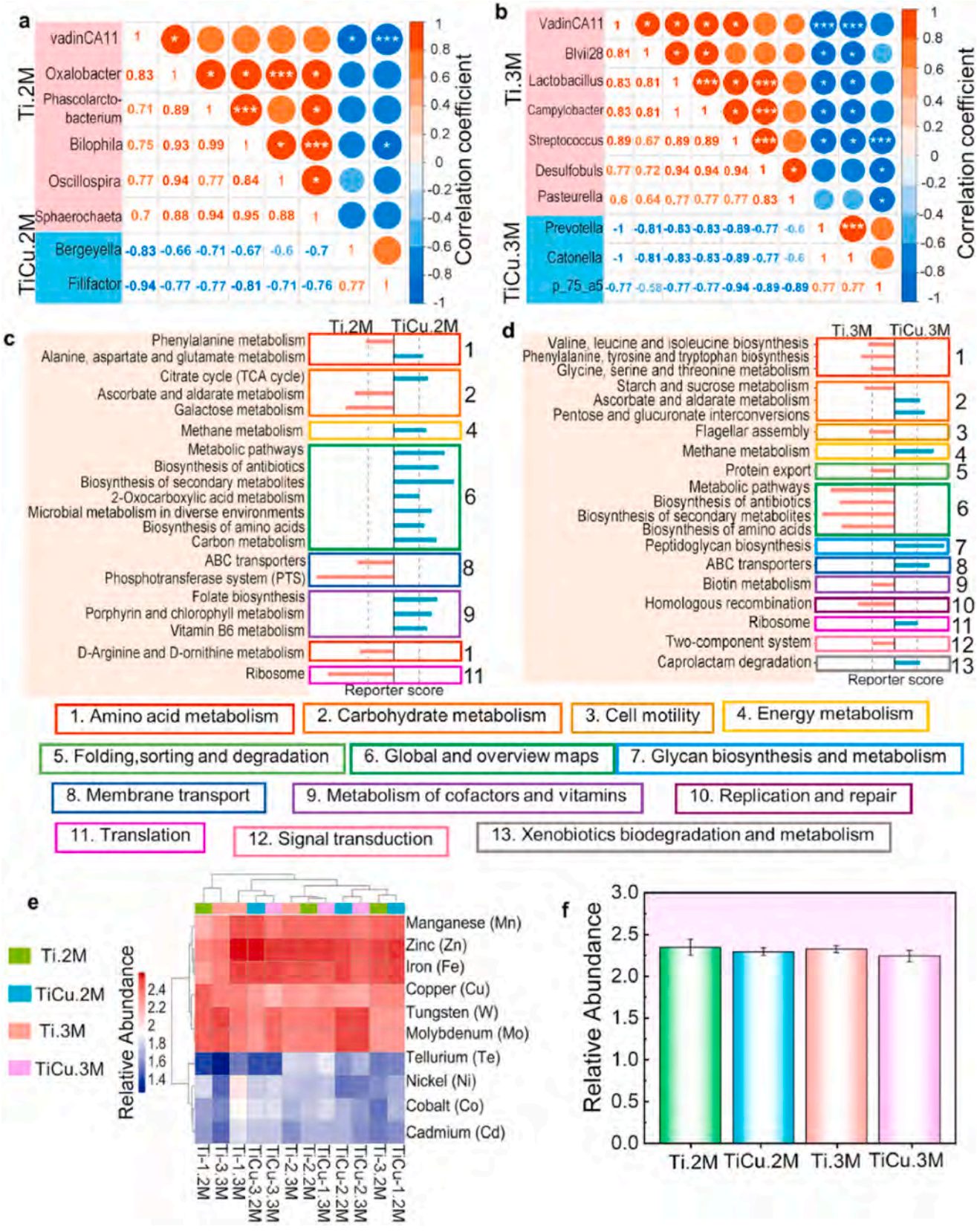

Fig. 5. Metagenomics analysis in the infection model. (a) and (b) correlation analysis of different genera at 2 M and 3 M, red circles showing positive correlations, and blue circles showing negative relationships. (c) and (f) Different metabolisms at 2 M and 3 M, pink and blue bars representing metabolism from the plaque on the Ti (scores < -1.65) and TiCu implants (scores > 1.65). (e) Heatmap analysis of metal resistance genes (top 10). (f) Relative abundance of Cu resistance gene ($n = 3$ per group) [Data are mean ± s.d.].

between the endogenous genera in the plaque of Ti and TiCu implants and were marked with blue circles, indicating that the endogenous genera of TiCu group were competitive against those of Ti group in all plaques.

3.2.7. Metabolism and resistant genes analysis

Metagenomic sequencing was used to study the effect of TiCu implant on the bacterial metabolism in the plaque microflora. At 2 M (Fig. 5c), among the amino acid metabolic pathways, phenylalanine metabolism was abundant in the microflora from the Ti group, while alanine, aspartate and glutamate metabolism were enriched in the microflora on the TiCu implant. Among the carbohydrate metabolic pathways, the citrate cycle, which only exists in aerobic respiration, was enriched in the plaque on TiCu implant. The plaque microflora on TiCu implant had an enrichment of cofactors and vitamin metabolic pathways, while membrane transport and translation pathways were abundant in the plaque on Ti implant.

As compared with 2 M, more metabolisms were detected in the microflora on Ti implant at the 3 M (Fig. 5d). For the amino acid metabolism, the microflora from Ti group were enriched in the glycine, serine, threonine, valine, leucine, isoleucine, phenylalanine, tyrosine and tryptophan biosynthesis pathways. For the carbohydrate metabolisms, starch and sucrose metabolism were abundant in the microflora from the Ti group, while the microflora from the TiCu group were enriched with pentose and glucuronate interconversions pathway, which are connected to the TCA cycle.

Finally, the metal resistance genes in the plaques were also analyzed in Fig. 5e, the abundances of Mn, Zn and Fe resistant genes were the highest among all the samples and there was also no significant difference in Cu resistance genes within the microflora from the Ti and TiCu groups at each month in Fig. 5f, which revealed that TiCu implant have no effect on the Cu resistance genes in the plaque.

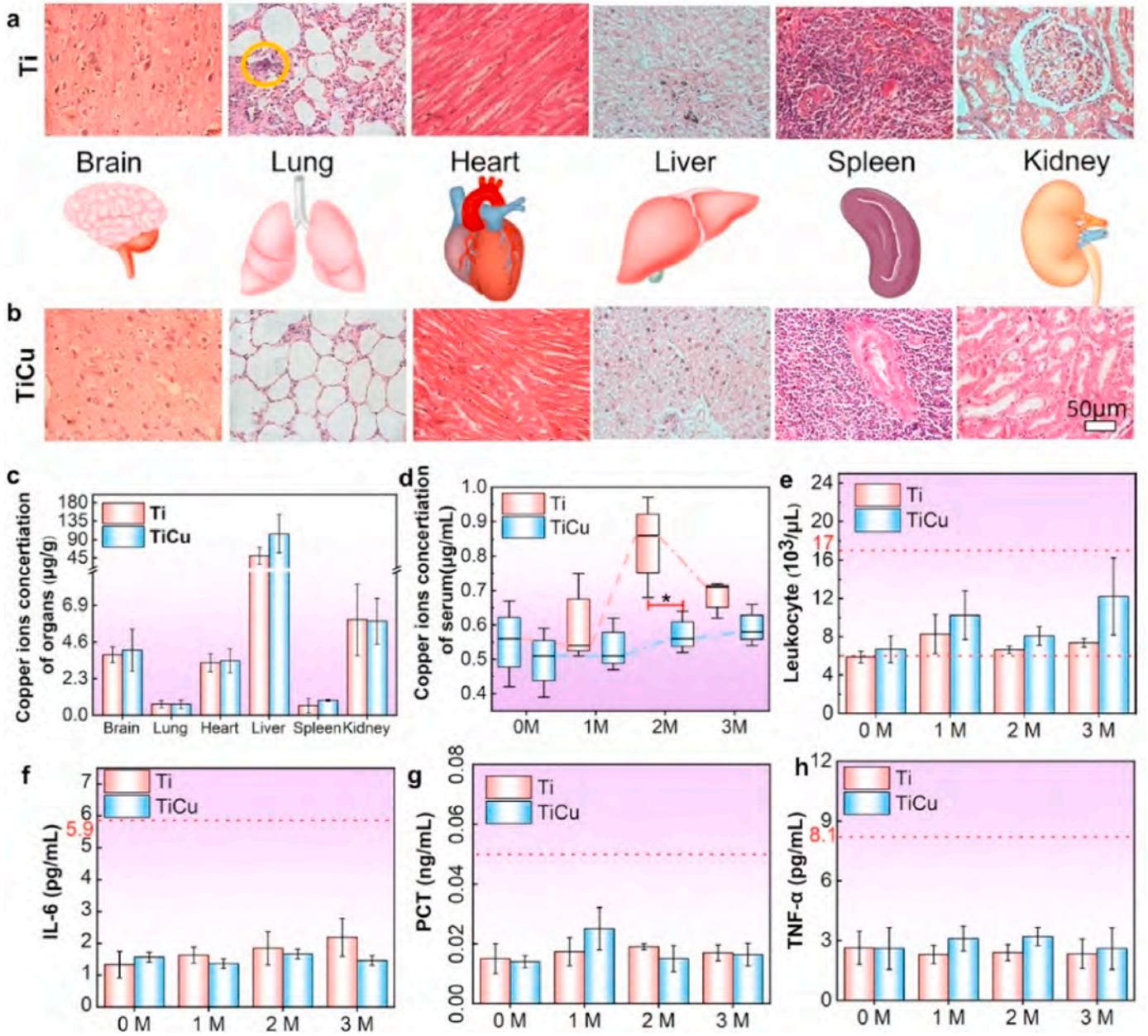

Fig. 6. Biosafety analysis in the infection model. (a) and (b) Histopathological analysis of major organs in animals with the Ti and TiCu implants, respectively. (c) Copper content in the major organs. (d) Copper content in the serum at each month. (e) Leukocytes. (f–h) Quantitative analysis of cytokines, including interleukin-6, tumor necrosis factor-α, and procalcitonin (n = 3 per group) [Data are mean ± s.d. and *p < 0.05 compared with the pure Ti implant].

3.2.8. Biosafety analysis of TiCu implant

Histopathological analyses on major organs in Ti and TiCu groups were performed by H&E staining (Fig. 6a and b), including brain, lung, heart, liver, spleen, and kidney. Except for the local inflammatory cell infiltration in the lungs of animals with Ti implants (yellow circle), the other organs were healthy in both groups, indicating good biosafety of TiCu implant.

Fig. 6c and d show the copper contents of the organs and serum. The copper content in the serum of animals with Ti implants was higher than that of animals with TiCu implants at 2 M. There were no significant differences among the organs or serum copper concentration during the other time periods. More than 90% of the copper in serum was in the ceruloplasmin, which is an acute-phase protein (APP). The level of APP was shown to increase with the development of infections [36,37]. The serum copper concentration was increased in the animals with Ti implants due to the peri-implant mucositis. The copper content in the major organs was highest in liver, followed by kidney, brain and heart, and then spleen and lung. These results were consistent with a previous study [36]. There were no significant differences in the copper content in the major organs between the two groups. Additionally, the number of leukocytes and cytokines in animals with Ti and TiCu implants were in the normal range at each time (Fig. 6e–h). These results indicated that both Ti and TiCu implants had good biosafety.

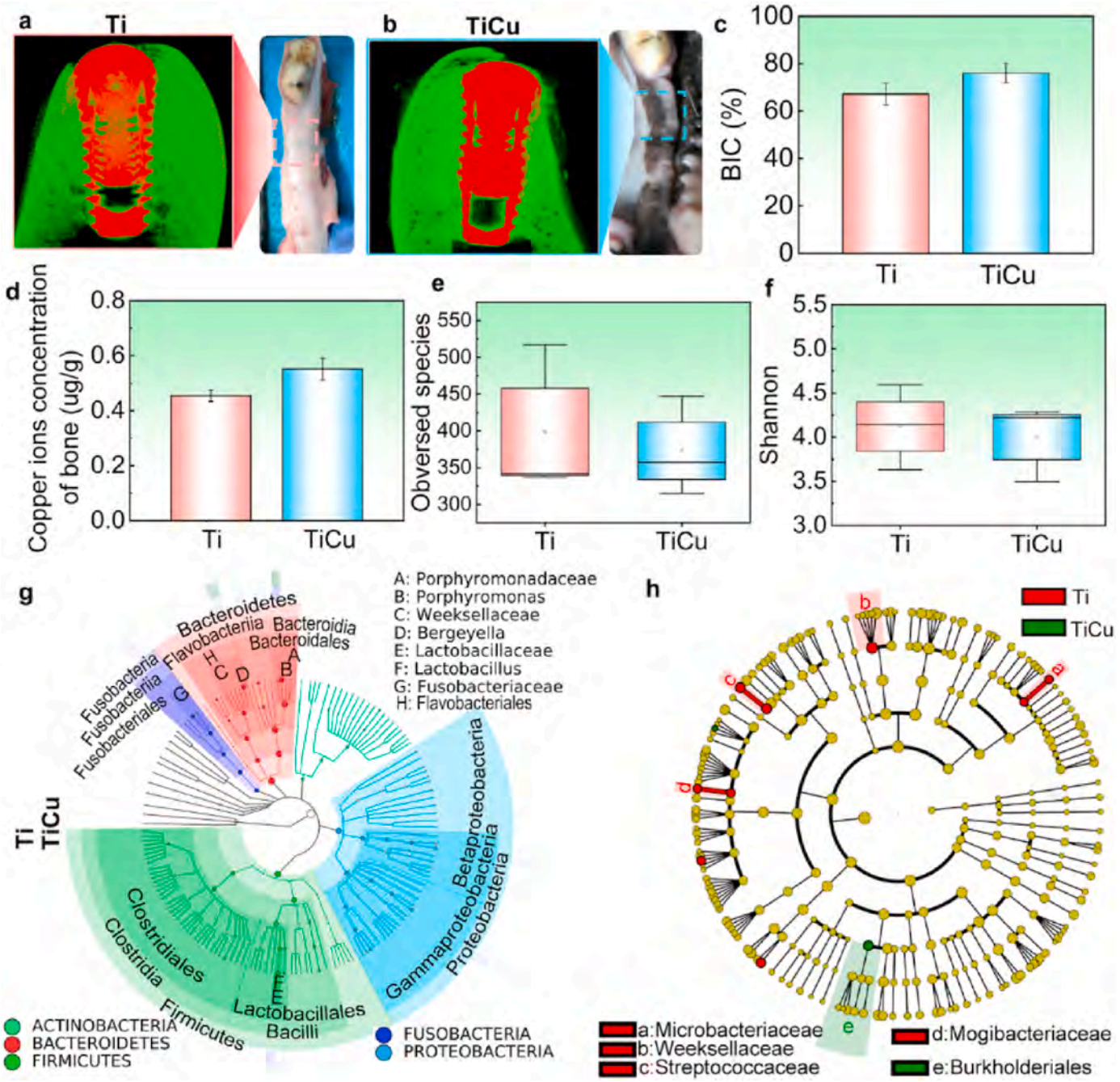

Fig. 7. Analysis in the normal implantation model. (a) and (b) Visual study and micro-CT images in animals with Ti and TiCu implants. (c) Quantitative analysis of BIC ratio. (d) Copper content in peri-implant bones. (e) Observed species analysis. (f) Shannon analysis. (g) Species composition tree of saliva samples. (h) LEfSe analysis of saliva microbiome profiles up to the genus level (n = 3 per group) [Data are mean ± s.d.].

3.3. Normal implantation model

In order to further value the biosafety of TiCu implant, the normal implantation model was developed, and general observations, micro-CT analysis, copper content evaluation and saliva microbiota were performed. The gums of the animals with Ti and TiCu implants were healthy with normal color, without bleeding or festers (Fig. 7a and b). The micro-CT images showed that numerous dense bone tissues spread around both Ti and TiCu implants without significant differences in the BIC rates between the two implants (Fig. 7c). The copper concentrations in the peri-implant bones were 0.45 μg/g and 0.55 μg/g for animals with Ti and TiCu implants, respectively (Fig. 7d). All these results indicated that both Ti and TiCu implants demonstrated suitable osseointegration and biosafety.

In the normal implantation model, saliva samples were harvested to explore the effect of TiCu implant on the oral microbiome. The taxonomic compositions of saliva samples included 11 phyla, 16 classes, 22 orders, 52 families, and 67 genera. Herein, Firmicutes, Proteobacteria, Bacteroidetes, Fusobacteria, and Actinobacteria were the most abundant phyla in all the samples (Fig. 7g). The alpha diversities of the saliva microflora from animals with Ti and TiCu implants were also no significant differences ($P > 0.05$, Fig. 7e and f), which further revealed the similarity between the saliva microbial compositions of animals with Ti and TiCu implants in the normal implantation model. Significantly different species between the two groups were also analyzed (Fig. 7h). The saliva microflora from the animals with Ti implants enriched Micriobacteriaceae, Weeksellaceae, Streptococcaceae and Mogibacteriaceae, while the abundance of Burkholderiales was higher in the microflora of animals with TiCu implants.

4. Discussion

With widely applications of dental implants, good osteointegration and sufficiently anti-infection ability are most desired to combat the implant-associated infections in clinic. While most researchers used single-pathogen induced infection models to assess the anti-infective implants [38,39], which neglected the effect of oral microbiome on the peri-implant infections. In this study, we combined the classical ligature induced peri-implant infection model with the sucrose-rich diet to explore the anti-infection mechanism and the biosafety of TiCu implant from the oral microbiology to peri-implant and organ tissues.

4.1. Anti-infection mechanism of TiCu alloy implant from the oral microbiology in the infection model

In the infection model, the visual assessment and histopathological analysis (Figs. 2 and 3) suggested that animals with Ti implants presented peri-implant mucositis. In contrast, animals with TiCu implants had healthy peri-implant tissues, which proved the anti-infective ability of TiCu implant in the oral infectious environment. Then we investigated the anti-infective mechanism of TiCu implant based on the plaque microbiology.

At the genus level of plaque microflora, only anaerobic bacteria were enriched in Ti implant surface at 2 M (Fig. 4e), including acidogenic bacteria and methanogens with obvious symbiotic relationships (Fig. 5a). Among them, both *Sphaerochaeta* and Synergistaceae were reported to be abundant in the plaque of patients with peri-implant mucositis and peri-implantitis [40]. At 3 M (Fig. 4f), pathogens, including *Pasteurella* and *Campylobacter*, acidogenic bacteria, and methanogens were obviously abundant in Ti group, where *Lactobacillus* and *Streptococcus* have been reported to generate lactic acid, which can be utilized by *Desulfobulbus* [41]. *Blvii28* has been demonstrated to metabolize sugars into hydrogen under anaerobic conditions, and *vadinCA11* utilizes hydrogen as an electron donor to produce methane [42]. These symbiotic bacteria could cooperatively acidify the plaque environment on Ti implant, and these disrupted microflora in the animals with Ti implants caused peri-implant mucositis to occur. In contrast, the endogenous microbiota on the TiCu implant surface at 2 M included *Bergeyella*, an aerobic bacterium and a dominant group in the healthy canine mouths [43], as well as *Filifactor*, an anaerobic bacterium that commonly colonizes the healthy periodontium [44]. At 3 M, the endogenous bacteria in animals with TiCu implants included *Prevotella*, a core group in gingival sulcus [45], *Catonella*, an anaerobe, and *p_75_a5*, a facultative anaerobe. These results suggested that TiCu implant can still maintain the oral microbiota balance in the infection model.

Except for the analysis of the dental plaque microflora, this work also investigated the effect of TiCu implant on the metabolisms at the gene level, thereby revealing the anti-infective mechanism of TiCu implant. The metabolism supports the growth and survival of microbiota [46], and carbohydrate metabolism fuels cellular activities with carbon and energy. The starch, sucrose and galactose metabolic pathways, whose products can be utilized by the endogenous anaerobes to acidify the plaque, were plentiful in the microflora attached to Ti implant (Fig. 5c and d). For instance, D-glyceraldehyde 3-phosphate and alpha-D-glucose 6-phosphate participate in the pentose phosphate pathway (HMP) and glycolytic pathway (EMP), and generate the acidic by-products [47]. However, the microflora formed on TiCu implant surface metabolized carbohydrates via the TCA cycle and generated plenty of ATP, and the citrate cycle is the well-known pathway in aerobic respiration [47], which is consistent with the aerobic microflora on the surface of TiCu implant.

In addition to the carbohydrate metabolism, some anaerobic and acidogenic bacteria can also ferment the amino acid via the gluconeogenic pathway to produce acids. For instance, the acid-producing capability of the microbiota isolated from dental caries increased with the content of several amino acids, including valine, leucine, isoleucine, phenylalanine, tyrosine, and tryptophan [48]. Notably, these amino acids significantly accumulated in the microflora from Ti implant (Fig. 5c and d), which acidified the plaques. Moreover, phosphotransferase system [49] is a vital acid-producing pathway of *Streptococcus* found in the plaque on Ti implant as well. The flagellar assembly pathway is associated with motile bacteria, such as *Sphaerochaeta*, and flagella are involved in not only the motility and chemotaxis, but also the secretion of virulence proteins [50]. Similarly, the protein export pathway is probably related to *Pasteurella* [51], which can release toxins into the plaque on the Ti implant. In contrast, TiCu implant sustained the metabolic balance of the microflora, including the metabolism of methane, cofactors and vitamins. Copper ions released from TiCu implant can boost Proteobacteria and Verrucomicrobia to utilize the methane, which prevents the formation of complete anaerobic plaque [52]. Moreover, the microbiota attached on TiCu implant was able to biosynthesize the folate, which is a methyl donor and nucleotide synthesis source for both the microbiota and the host [53]. Additionally, copper is an essential element for complex IV of the electron transport chain, as it forms Cu-porphyrin [54], we also found that TiCu implant enriched the metabolism of porphyrin and chlorophyll to promote the aerobic respiration in the microflora, as shown in Fig. 5c and d.

Based on the above analysis, we summarized the underlying anti-infection mechanism of TiCu implants, which was shown in Fig. 8. In the infection model, the endogenous species in the microflora on the surface of Ti and TiCu implants led to significant differences in the carbohydrate metabolism, as the results of the sucrose-rich diets. In the plaque on Ti implant, anaerobes produced acids to acidify the microenvironments, which was also advantageous for the accumulations of acidogenic bacteria and pathogens. As dysbiosis occurred, the bacteria eventually colonized and infected in the peri-implant tissues, causing peri-implant disease in animals. In contrast, TiCu implant maintained the metabolic balance and prevented the formation of the acidic environment, and at the microflora level, TiCu implant preserved the balance of anaerobes and aerobes, thus maintaining the health of the peri-implant tissues and preventing the formation of the peri-implant diseases.

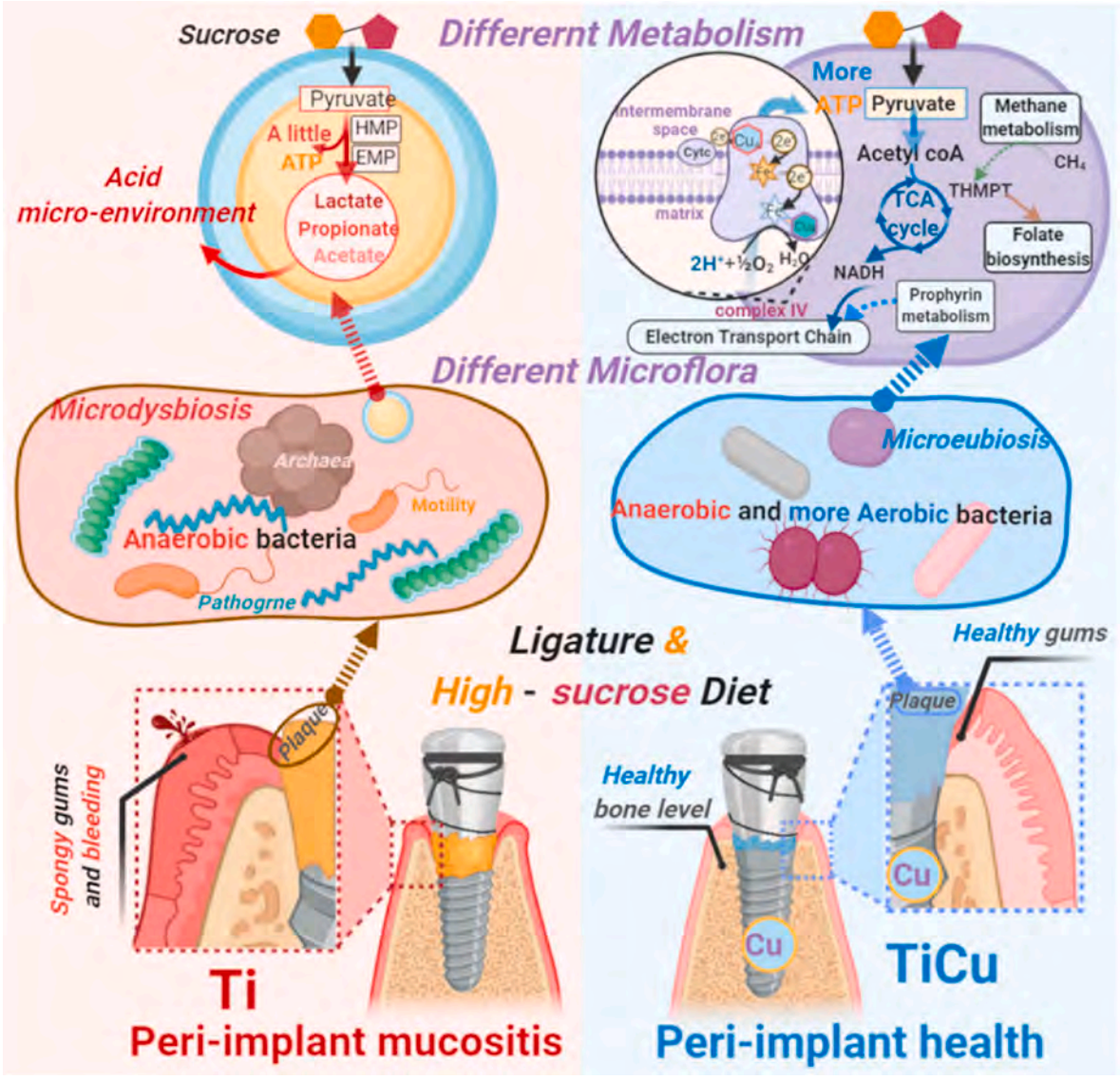

Fig. 8. Schematic representation for anti-infective mechanism of TiCu implant in the ligature and sucrose-rich diet-induced model. The microflora in animals with Ti implant metabolized the sucrose to acidify the environment and disturb the plaque microflora, and this microdysbiosis resulted in the peri-implant mucositis to occur. While the microflora on the TiCu implant sustained a metabolic balance, avoiding the acid plaque and maintaining the microflora balance of aerobic and anaerobic bacteria. TiCu implant preserved healthy peri-implant tissues. This diagram was created with BioRender.com.

4.2. Effect of TiCu implant on the saliva microflora in the normal implantation model

The effect of TiCu implant on the saliva microbiome was examined in the normal implantation model due to the local environment in the mouth communicated with one another via saliva [55]. The core microbiota and diversity of the saliva microflora were similar between the animals with Ti and TiCu implants (Fig. 7). Among the endogenous species in the saliva of animals with Ti implants, Mogibacteriaceae was previously related with an extraoral abscess [56], Streptococcaceae was an acidogenic bacteria, and both Micriobacteriaceae and Weeksellaceae were identified in the mouth of healthy dogs [57]. Additionally, salvia from animals with TiCu implants was enriched with Burkholderiales, whose member, *Burkholderia cepacian*, is a pathogen associated with skin infections [58]. All animals in the normal model were healthy without skin and peri-implant diseases. Based on the analyses of the histology and the saliva microbiome, both Ti and TiCu implants kept the balance of the saliva microbiota, maintained the health of the peri-implant tissues, and promoted good osseointegrations between the bone and implant.

4.3. Biosafety analysis of TiCu implant

Titanium implants have been commonly used due to their excellent biocompatibility, good mechanical properties, and high corrosion resistance. For instance, a 5-year retrospective clinical study showed that the Dentium implants have a cumulative survival rate of up to 97.37% [59]. Therefore, Dentium implants were chosen as the control group in this study. A previous study demonstrated that TiCu alloy possessed higher strength and better corrosion resistance [27], which is a predominant factor for long-term service in the human body. Biosafety is a critical factor for future clinical applications. As following, the biosafety of TiCu implant was comprehensively discussed on the compatibility and the health of the peri-implant tissues, as well as the blood markers and major organ histology, the systemic distribution of copper content, and the influence of metal resistance genes.

(1) Compatibility of peri-implant tissues: BIC is an indicator for stability and osseointegration of a bone implant [18]. BIC of the TiCu implant was higher than that of the Ti implant in both models, without significantly differences. These results demonstrated that TiCu implant possessed the same osseointegration ability as the clinically used implant. Furthermore, TiCu implant was able to inhibit peri-implant mucositis in the infection model. TiCu implant also maintained the balance of the saliva microbiome in the normal implantation model, and thus maintained the health of the peri-implant tissue. Taken together, the excellent compatibility of the TiCu implant could be confirmed.
(2) Biosafety of the implant in the blood and major organs: Histological analyses of the brain, lung, heart, liver, spleen, and kidney in animals with TiCu implants showed that all the organs were healthy without inflammatory cell infiltrations. Additionally, both leukocytes and cytokine levels were in the normal range, which suggested that the animals did not become infected with systemic diseases. These results demonstrated a suitable biosafety of TiCu implant.
(3) Copper content distribution: Several researchers have shown that Cu-containing biomaterials have excellent antibacterial activity, as well as vascularization and osseointegration effects [60]. Meanwhile, concerns about the effect of Cu-containing biomaterials on the copper distribution in the tissues have also been attracted. In this study, the copper content in the bone tissues around the TiCu implant was slightly higher than that around the Ti implant in the normal implantation model, which was contributed to the osteogenic effect of the TiCu implant [13]. Moreover, in the infection model, the copper contents in major organs were similar between animals with Ti and TiCu implants, respectively, and the copper distribution was consistent with a study showing the copper distribution sequence in human organs [36], revealing that the copper released from the TiCu implant was safe to the hosts.
(4) Influence of metal resistance genes: In the infection model, the microflora from the plaque on TiCu implant had similar level of metal resistance gene abundances (including copper) as compared to the microflora from animals with Ti implants. This demonstrated that TiCu implant did not disturb the balance of resistance genes or affect the generation and transmission of copper resistance genes among oral microflora.

Dental implants with anti-infection functions have been increasingly investigated in recent years, however, the widely used single-pathogen induced infection animal models take no consideration into the effect of oral microflora. In this study, we made considerable progress to create an infective environment using the native oral bacteria to determine the anti-infective mechanism of the TiCu implant. The results showed that the TiCu implant could maintain the oral microbiota homeostasis to suppress peri-implant inflammatory response, and also possessed good biosafety. In the further work, we will try much more effort to explore the effect of Cu ions on the TCA cycle using molecular biotechnology, in order to further understand the mechanism of TiCu implant on the microflora balance of aerobic and anaerobic bacteria in oral environment.

5. Conclusion

This work created an infective environment by native oral bacteria in a ligature and sucrose-rich diets induced dog model. Further we explored the anti-infection mechanism of TiCu implants by 16S rRNA gene and metagenomic sequences to estimate the effect of TiCu implant on the oral microecology. The results revealed that TiCu implants promoted carbohydrate metabolism via the TCA cycle in the oral microbiota, which avoided the formation of acidic plaque. TiCu implants also maintained the balance of anaerobes and aerobes, as such, the peri-implant tissues remained healthy. In the normal implantation model, TiCu implants also maintained the balance of the saliva microbiome to preserve peri-implant health. Additionally, the biosafety of TiCu implants was demonstrated via the analysis of tissue compatibility and released copper content, as well as the analysis of copper resistance genes. Thereby this study provided a novel insight into the development of antibacterial metal implants.

CRediT authorship contribution statement

Hui Liu: Methodology, Writing – original draft, Visualization, Project administration. **Yulong Tang:** Investigation, Validation, Project administration. **Shuyuan Zhang:** Resources, Project administration. **Huan Liu:** Visualization, Project administration. **Zijian Wang:** Project administration. **Yue Li:** Project administration. **Xinluan Wang:** Writing – review & editing. **Ling Ren:** Conceptualization, Methodology, Writing – review & editing, Supervision, Funding acquisition. **Ke Yang:** Conceptualization, Writing – review & editing, Supervision, Funding acquisition. **Ling Qin:** Writing – review & editing, Supervision, Funding acquisition.

Declaration of competing interest

The authors declare that they have no known competing financial interests or personal relationships that could have appeared to influence the work reported in this paper.

Acknowledgments

This work was supported by the Bureau of International Cooperation, Chinese Academy of Sciences [174321KYSB20180006]; National Key Research and Development Program of China [2018YFC1106600, 2016YFC1100600]; Natural Science Foundation of China [51631009, 31870954]; and Liaoning Revitalization Talents Program [XLYC1807069]. The authors especially thankful for the assistance from Chuanshi Sui (Shenyang SYRICIT Testing Co., Ltd.) on the bioinformation analysis of 16S rRNA gene sequencing and metagenomic sequencing. The authors also thank LetPub (www.letpub.com) for its linguistic assistance during the preparation of this manuscript.

References

[1] S. Jayachandran, A.D. Walmsley, K. Hill, Challenges in dental implant provision and its management in general dental practice, J. Dent. 99 (2020) 103414, https://doi.org/10.1016/j.jdent.2020.103414.
[2] O.Z. Andersen, V. Offermanns, M. Sillassen, K.P. Almtoft, I.H. Andersen, S. Sørensen, C.S. Jeppesen, D.C.E. Kraft, J. Bøttiger, M. Rasse, F. Kloss, M. Foss, Accelerated bone ingrowth by local delivery of strontium from surface functionalized titanium implants, Biomaterials 24 (2013) 5883–5890, https://doi.org/10.1016/j.biomaterials.2013.04.031.
[3] C.T. Lee, Y.W. Huang, L. Zhu, R. Weltman, Prevalences of peri-implantitis and peri-implant mucositis: systematic review and meta-analysis, J. Dent. 62 (2017) 1–12, https://doi.org/10.1016/j.jdent.2017.04.011.
[4] G. Subbiahdoss, R. Kuijer, D.W. Grijpma, H.C. van der Mei, H.J. Busscher, Microbial biofilm growth vs. tissue integration: "The race for the surface" experimentally studied, Acta Biomater. 5 (2009) 1399–1404, https://doi.org/10.1016/j.actbio.2008.12.011.
[5] I. Burghardt, F. Lüthen, C. Prinz, B. Kreikemeyer, C. Zietz, H.-G. Neumann, J. Rychly, A dual function of copper in designing regenerative implants, Biomaterials 44 (2015) 36–44, https://doi.org/10.1016/j.biomaterials.2014.12.022.
[6] M.K. Narbat, B.F.L. Lai, C. Ding, J.N. Kizhakkedathu, R.E.W. Hancock, R. Wang, Multilayered coating on titanium for controlled release of antimicrobial peptides for the prevention of implant-associated infections, Biomaterials 34 (2013) 5969–5977, https://doi.org/10.1016/j.biomaterials.2013.04.036.
[7] H. Chouirfa, H. Bouloussa, V. Migonney, C.F. Daudré, Review of titanium surface modification techniques and coatings for antibacterial applications, Acta Biomater. 83 (2019) 37–54, https://doi.org/10.1016/j.actbio.2018.10.036.
[8] M. Wang, T. Tang, Surface treatment strategies to combat implant-related infection from the beginning, J. Orthop. Transl. 17 (2019) 42–54, https://doi.org/10.1016/j.jot.2018.09.001.
[9] S.G. Rotman, K. Thompson, D.W. Grijpma, R.G. Richards, T.F. Moriarty, D. Eglin, O. Guillaume, Development of bone seeker–functionalised microspheres as a

targeted local antibiotic delivery system for bone infections, J.Orthop. Transl. 21 (2020) 136–145, https://doi.org/10.1016/j.jot.2019.07.006.
[10] X. Qu, H. Yang, B. Jia, Z. Yu, Y. Zheng, K. Dai, Biodegradable Zn-Cu alloys show antibacterial activity against MRSA bone infection by inhibiting pathogen adhesion and biofilm formation, Acta Biomater. 117 (2020) 400–417, https://doi.org/10.1016/j.actbio.2020.09.041.
[11] J. Yang, H. Qin, Y. Chai, P. Zhang, Y. Chen, K. Yang, M. Qin, Y. Zhang, H. Xia, L. Ren, B. Yu, Molecular mechanisms of osteogenesis and antibacterial activity of Cu-bearing Ti alloy in a bone defect model with infection in vivo, J. Orthop. Transl. 27 (2020) 77–89, https://doi.org/10.1016/j.jot.2020.10.004.
[12] R. Liu, K. Memarzadeh, B. Chang, Y. Zhang, Z. Ma, R.P. Allaker, L. Ren, K. Yang, Antibacterial effect of copper-bearing titanium alloy (Ti-Cu) against Streptococcus mutans and Porphyromonas gingivalis, Sci. Rep. 6 (2016) 29985, https://doi.org/10.1038/srep29985.
[13] R. Liu, Y. Tang, H. Liu, L. Zeng, Z. Ma, J. Li, Y. Zhao, L. Ren, K. Yang, Effects of combined chemical design (Cu addition) and topographical modification (SLA) of Ti-Cu/SLA for promoting osteogenic, angiogenic and antibacterial activities, J. Mater. Sci. Technol. 47 (2020) 202–215, https://doi.org/10.1016/j.jmst.2019.10.045.
[14] R. Liu, Y. Tang, L. Zeng, Y. Zhao, Z. Ma, Z. Sun, L. Xiang, L. Ren, K. Yang, In vitro and in vivo studies of anti-bacterial copper-bearing titanium alloy for dental application, Dent. Mater. 34 (2018) 1112–1126, https://doi.org/10.1016/j.dental.2018.04.007.
[15] M. Badar, M.I. Rahim, M. Kieke, T. Ebel, M. Rohde, H. Hauser, P. Behrens, P. P. Mueller, Controlled drug release from antibiotic-loaded layered double hydroxide coatings on porous titanium implants in a mouse model, J. Biomed. Mater. Res., Part A. 103 (2015) 2141–2149, https://doi.org/10.1002/jbm.a.35358.
[16] C.X. Zhou, L. Li, Y.G. Ma, B.N. Li, G. Li, Z. Zhou, F. Shi, J. Weng, C. Zhang, F. Wang, X. Cui, L. Wang, H. Wang, A bioactive implant in situ and long-term releases combined drugs for treatment of osteoarticular tuberculosis, Biomaterials 176 (2018) 50–59, https://doi.org/10.1016/j.biomaterials.2018.05.039.
[17] J.A. Aas, B.J. Paster, L.N. Stokes, I. Olsen, F.E. Dewhirst, Defining the normal bacterial flora of the oral cavity, J. Clin. Microbiol. 43 (2005) 5721–5732, https://doi.org/10.1128/JCM.43.11.5721-5732.2005.
[18] T. Berglundh, G. Armitage, M.G. Araujo, G.A. Ortiz, J. Blanco, P.M. Camargo, S. Chen, D. Cochran, J. Derks, E. Figuero, C.F. Hammerle, L.A. Heitz-Mayfield, G. Huynh-Ba, V. Iacono, K.T. Koo, F. Lambert, L. McCauley, M. Quirynen, S. Renvert, G.E. Salvi, F. Schwarz, D. Tarnow, C. Tomasi, H.L. Wang, N. Zitzmann, Peri-implant diseases and conditions: consensus report of workgroup 4 of the 2017 world workshop on the classification of periodontal and peri-implant diseases and conditions, J. Clin. Periodontol. 89 (2018) S313–S318, https://doi.org/10.1111/jcpe.12957.
[19] A.E. Pinedo, J.F. Lopez, Beyond microbial community composition: functional activities of the oral microbiome in health and disease, Microb. Infect. 17 (2015) 505–516, https://doi.org/10.1016/j.micinf.2015.03.014.
[20] W.S. Borgnakke, IDF Diabetes Atlas: diabetes and oral health: a two-way relationship of clinical importance, Diabetes Res. Clin. Pract. 157 (2019) 107839, https://doi.org/10.1016/j.diabres.2019.107839.
[21] M.P. Molina, J.L. Martinez, F. O'Valle, P.G. Moreno, Microbial profiles and detection techniques in peri-implant diseases: a systematic review, J. Oral Maxillofac. Res. 7 (2016) e10, https://doi.org/10.5037/jomr.2016.7310.
[22] F. Melo, F.C. Milanesi, P.D. Angst, R.V. Oppermann, A systematic review of the microbiota composition in various peri-implant conditions: data from 16S rRNA gene sequencing, Arch. Oral Biol. 117 (2020) 104776, https://doi.org/10.1016/j.archoralbio.2020.104776.
[23] L.D. Alcaraz, P.B. Ferre, R.C. Rubio, H. Romero, A.S. Soro, M. Pignatelli, A. Mira, Identifying a healthy oral microbiome through metagenomics, Clin. Microbiol. Infect. 18 (2012) 54–57, https://doi.org/10.1111/j.1469-0691.2012.03857.x.
[24] J.G.S. Souza, M.M. Bertolini, R.C. Costa, B.E. Nagay, A.D. Bagtzoglou, V.R. Barão, Targeting implant-associated infections: titanium surface loaded with antimicrobial, iScience 24 (2021) 102008, https://doi.org/10.1016/j.isci.2020.102008, 102008.
[25] H. Koo, M.L. Falsetta, M.I. Klein, The exopolysaccharide matrix: a virulence determinant of cariogenic biofilm, J. Dent. Res. 92 (2013) 1065–1073, https://doi.org/10.1177/0022034513504218.
[26] J. Xiao, M.I. Klein, M.L. Falsetta, B. Lu, C.M. Delahunty, J.R. Yates 3rd, A. Heydorn, H. Koo, The exopolysaccharide matrix modulates the interaction between 3D architecture and virulence of a mixed-species oral biofilm, PLoS Pathog. 8 (2012), e1002623, https://doi.org/10.1371/journal.ppat.1002623 e1002623.
[27] J. Wang, S. Zhang, Z. Sun, H. Wang, L. Ren, K. Yang, Optimization of mechanical property, antibacterial property and corrosion resistance of Ti-Cu alloy for dental implant, J. Mater. Sci. Technol. 35 (2019) 2336–2344, https://doi.org/10.1016/j.jmst.2019.03.044.
[28] Y.H. An, R.J. Friedman, Animal models of orthopedic implant infection, J. Invest. Surg. 11 (1998) 139–146, https://doi.org/10.3109/08941939809032193.
[29] U.D. Ramos, F.A. Suaid, U.M. Wikesjö, C. Susin, M. Taba Jr., A.B. Novaes Jr., Comparison between two antimicrobial protocols with or without guided bone regeneration in the treatment of peri-implantitis. A histomorphometric study in dogs, Clin. Oral Implants Res. 28 (2017) 1388–1395, https://doi.org/10.1111/clr.12998.
[30] K. Aagaard, J. Petrosino, W. Keitel, M. Watson, J. Katancik, N. Garcia, S. Patel, M. Cutting, T. Madden, H. Hamilton, E. Harris, D. Gevers, G. Simone, P. McInnes, J. Versalovic, The Human Microbiome Project strategy for comprehensive sampling of the human microbiome and why it matters, Faseb. J. 27 (2013) 1012–1022, https://doi.org/10.1096/fj.12-220806.
[31] P.D. Schloss, S.L. Westcott, T. Ryabin, J.R. Hall, M. Hartmann, E.B. Hollister, R. A. Lesniewski, B.B. Oakley, D.H. Parks, C.J. Robinson, J.W. Sahl, B. Stres, G. G. Thallinger, D.J. Van Horn, C.F. Weber, Introducing mothur: open-source, platform-independent, community-supported software for describing and comparing microbial communities, Appl. Environ. Microbiol. 75 (2009) 7537–7541, https://doi.org/10.1128/AEM.01541-09.
[32] Y. Chen, SOAPnuke: a MapReduce acceleration-supported software for integrated quality control and preprocessing of high-throughput sequencing data, GigaScience 7 (2018) 1–6, https://doi.org/10.1093/gigascience/gix120.
[33] L. Fu, B. Niu, Z. Zhu, S. Wu, W. Li, CD-HIT, Accelerated for clustering the next-generation sequencing data, Bioinformatics 28 (2012) 3150–3152, https://doi.org/10.1093/bioinformatics/bts565.
[34] A. Wennerberg, T. Albrektsson, Effects of titanium surface topography on bone integration: a systematic review, Clin. Oral Implants Res. 4 (2009) 172–184, https://doi.org/10.1111/j.1600-0501.2009.01775.x.
[35] S. Renvert, G.R. Persson, F.Q. Pirih, P.M. Camargo, Peri-implant health, peri-implant mucositis, and peri-implantitis: case definitions and diagnostic considerations, J. Clin. Periodontol. 89 (2018) S304–S312, https://doi.org/10.1111/jcpe.12956.
[36] P. Zatta, A. Frank, Copper deficiency and neurological disorders in man and animals, Brain Res. Rev. 54 (2007) 19–33, https://doi.org/10.1016/j.brainresrev.2006.10.001.
[37] J. Rogers, D. Lahiri, Metal and inflammatory targets for alzheimers disease, Curr. Drug Targets 5 (2004) 535–551, https://doi.org/10.1016/10.2174/1389450043345272.
[38] R.M.Y. Wong, T. Li, J. Li, W.T. Ho, S.K.H. Chow, S.S.Y. Leung, W.H. Cheung, M. Ip, A systematic review on current osteosynthesis-associated infection animal fracture models, J. Orthop. Transl. 23 (2020) 8–20, https://doi.org/10.1016/j.jot.2020.03.002.
[39] S. Sebastian, Y. Liu, R. Christensen, D.B. Raina, M. Tägil, L. Lidgren, Antibiotic containing bone cement in prevention of hip and knee prosthetic joint infections: a systematic review and meta-analysis, J. Orthop. Transl. 23 (2020) 53–60, https://doi.org/10.1016/j.jot.2020.04.005.
[40] J.A. Shibli, L. Melo, D.S. Ferrari, L.C. Figueiredo, M. Faveri, M. Feres, Composition of supra- and subgingival biofilm of subjects with healthy and diseased implants, Clin. Oral Implants Res. 19 (2008) 975–982, https://doi.org/10.1111/j.1600-0501.2008.01566.x.
[41] J. Kuever, F.A. Rainey, F. Widdel, Desulfobulbus, in: S.E. Trujillo, P. DeVos, B. Hedlund, P. Kämpfer, F.A. Rainey, W.B. Whitman (Eds.), Bergey's Manual of Systematics of Archaea and Bacteria, John Wiley & Sons, Ltd, Chichester, 2015, pp. 1–6.
[42] F. Matarazzo, A.C. Ribeiro, M. Faveri, C. Taddei, M.B. Martinez, M.P.A. Mayer, The domain Archaea in human mucosal surfaces, Clin. Microbiol. Infect. 18 (2012) 834–840, https://doi.org/10.1111/j.1469-0691.2012.03958.x.
[43] A. Sturgeon, J.W. Stull, M.C. Costa, J.S. Weese, Metagenomic analysis of the canine oral cavity as revealed by high-throughput pyrosequencing of the 16S rRNA gene, Vet. Microbiol. 162 (2013) 891–898, https://doi.org/10.1016/j.vetmic.2012.11.018.
[44] J.S. Lee, R. Spooner, N. Chowdhury, V. Pandey, B. Wellslager, K.R. Atanasova, Z. Evans, Ö. Yilmaz, In situ intraepithelial localizations of opportunistic pathogens, porphyromonas gingivalis and filifactor alocis, in human gingiva, Curr. Res. Microb. Sci. 1 (2020) 7–17, https://doi.org/10.1016/j.crmicr.2020.05.001.
[45] M. Gürsoy, I. Harju, J. Matomäki, A. Bryk, E. Könönen, Performance of MALDI-TOF MS for identification of oral Prevotella species, Anaerobe 47 (2017) 89–93, https://doi.org/10.1016/j.anaerobe.2017.04.008.
[46] V. Chubukov, L. Gerosa, K. Kochanowski, U. Sauer, Coordination of microbial metabolism, Nat. Rev. Microbiol. 12 (2014) 327–340, https://doi.org/10.1038/nrmicro3238.
[47] N. Takahashi, J. Washio, G. Mayanagi, Metabolomic approach to oral biofilm characterization—a future direction of biofilm research, J. Oral Biosci. 54 (2012) 138–143, https://doi.org/10.1016/j.job.2012.02.005.
[48] S. Dreizen, J.J. Mosny, E.J. Gilley, T.D. Spies, The amino acid requirements of oral acidogenic microorganisms associated with human dental caries, J. Dent. Res. 33 (1954) 339–345, https://doi.org/10.1177/00220345540330030701.
[49] W.A. Pérez, A.F. Pérez, M.C. Pabón, Molecular docking and in silico studies of the physicochemical properties of potential inhibitors for the phosphotransferase system of Streptococcus mutans, Arch. Oral Biol. 98 (2019) 164–175, https://doi.org/10.1016/j.archoralbio.2018.09.020.
[50] P. Guerry, Campylobacter flagella: not just for motility, Trends Microbiol. 15 (2007) 456–461, https://doi.org/10.1016/j.tim.2007.09.006.
[51] R. Hurtado, D. Carhuaricra, S. Soares, M.V.C. Viana, V. Azevedo, L. Maturrano, F. Aburjaile, Pan-genomic approach shows insight of genetic divergence and pathogenic-adaptation of Pasteurella multocida, Gene 670 (2018) 193–206, https://doi.org/10.1016/j.gene.2018.05.084.
[52] J.D. Semrau, A.A. DiSpirito, W. Gu, S. Yoon, Metals and methanotrophy, Appl. Environ. Microbiol. 84 (2018) 17, https://doi.org/10.1128/AEM.02289-17, e02289.
[53] H.K. Biesalski, Nutrition meets the microbiome: micronutrients and the microbiota, Ann. N. Y. Acad. Sci. 1372 (2016) 53–64, https://doi.org/10.1111/nyas.13145.
[54] B.E. Kim, T. Nevitt, D.J. Thiele, Mechanisms for copper acquisition, distribution and regulation, Nat. Chem. Biol. 4 (2008) 176–185, https://doi.org/10.1038/nchembio.72.
[55] J.M. Welch, S.T. Puebla, G. Borisy, Oral microbiome geography: micron-scale habitat and niche, Cell Host Microbe 28 (2020) 160–168, https://doi.org/10.1016/j.chom.2020.07.009.

[56] F. Nakazawa, M. Sato, S.E. Poco, T. Hashimura, T. Ikeda, S. Kalfas, G. Sundqvist, E. Hoshino, Description of Mogibacterium pumilum gen. nov., sp. nov. and Mogibacterium vescum gen. nov., sp. nov., and reclassification of Eubacterium timidum (Holdeman et al. 1980) as Mogibacterium timidum gen. nov., comb. nov, Int. J. Syst. Evol. Microbiol. 50 (2000) 679–688, https://doi.org/10.1099/00207713-50-2-679.

[57] Z. He, A. Isaiah, A.R. Hoffmann, R. Kelley, P. Mundell, J.M. Steiner, J. S. Suchodolski, Characterization of the nasal and oral microbiota of detection dogs, PloS One 12 (2017), e0184899, https://doi.org/10.1371/journal.pone.0184899.

[58] C.L. Cain, S.D. Cole, C.W. Bradley Ii, M.S. Canfield, E.A. Mauldin, Clinical and histopathological features of Burkholderia cepacia complex dermatitis in dogs: a series of four cases, Vet. Dermatol. 29 (2018) e156, https://doi.org/10.1111/vde.12677, e457.

[59] J.Y. Lee, H.J. Park, J.H. Kim, Y.G. Choi, Y.S. Kim, J.B. Huh, S.W. Shin, A 5-year retrospective clinical study of the Dentium implants, J. Adv. Prosthodont. 3 (2011) 229–235, https://doi.org/10.4047/jap.2011.3.4.229.

[60] A. Jacobs, G. Renaudin, C. Forestier, J.M. Nedelec, S. Descamps, Biological properties of copper-doped biomaterials for orthopedic applications: a review of antibacterial, angiogenic and osteogenic aspects, Acta Biomater. 117 (2020) 21–39, https://doi.org/10.1016/j.actbio.2020.09.044.